ACS APPLIED MATERIALS & INTERFACES

Research Article

www.acsami.org

Superlow Thermal Conductivity 3D Carbon Nanotube Network for Thermoelectric Applications

Jikun Chen,[†,‡] Xuchun Gui,*[,‡,§,⊥] Zewei Wang,[†] Zhen Li,[⊥] Rong Xiang,[§] Kunlin Wang,[⊥] Dehai Wu,[⊥] Xugui Xia,[†] Yanfei Zhou,[†] Qun Wang,[†] Zikang Tang,[§] and Lidong Chen[†,*]

[†]CAS Key laboratory of Materials for Energy Conversion, Shanghai Institute of Ceramics, Chinese Academy of Science, 1295 Dingxi Road, Shanghai 200050, PR China.

[§]State Key Lab of Optoelectronic Materials and Technologies, School of Physics and Engineering, Sun Yat-sen University, Guangzhou 510275, P. R. China

[⊥]Key Laboratory for Advanced Materials Processing Technology and Department of Mechanical Engineering, Tsinghua University, Beijing 100084, P. R. China

Supporting Information

ABSTRACT: Electrical and thermal transportation properties of a novel structured 3D CNT network have been systematically investigated. The 3D CNT net work maintains extremely low thermal conductivity of only 0.035 W/(m K) in standard atmosphere at room temperature, which is among the lowest compared with other reported CNT macrostructures. Its electrical transportation could be adjusted through a convenient gas-fuming doping process. By potassium (K) doping, the original p-type CNT network converted to n-type, whereas iodine (I_2) doping enhanced its electrical conductivity. The self-sustainable homogeneous network structure of as-fabricated 3D CNT network made it a promising candidate as the template for polymer composition. By in situ nanoscaled composition of 3D CNT network with polyaniline (PANI), the thermoelectric performance of PANI was significantly improved, while the self-sustainable and flexible structure of the 3D CNT network has been retained. It is hoped that as-fabricated 3D CNT network will contribute to the development of low-cost organic thermoelectric area.

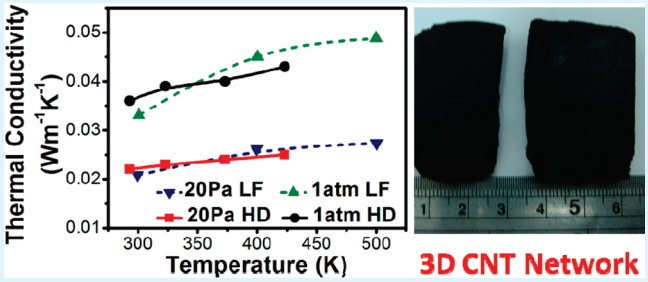

KEYWORDS: *CNT network, thermal conductivity, nanocompositing, thermoelectric*

1. INTRODUCTION

Nanoporous materials are a long sought-after class of materials in the seeking of lightweight, high porosity and large specific surface area materials. In recent years, different nanoporous materials have been fabricated such as nanoporous metal foams,[1] macroporous silicon,[2] porous graphene oxide macrostructure,[3,4] high porosity carbon nanotube (CNT) macrostructure.[5,6] Its unique structure and excellent properties demonstrated potential applications in a variety of areas such as catalytic materials,[1] organic thermoelectric materials,[7] mechanical energy absorption,[8−10] biomechanics,[11] filtration, and separation.[12,13] In recent years, the development of organic thermoelectric material has received special attention because of its easy fabrication and low costs in potential applications to achieve conversion between thermal and electrical energy without moving mechanical components or hazardous working fluids.

Performance of a thermoelectric material is evaluated by a figure of merit, given by $ZT = S^2\sigma T/\kappa$, where S, σ, T, and κ are the thermopower, electrical conductivity, temperature, and thermal conductivity, respectively.[14−28] Conventionally, the parameters of S, σ, and κ of three-dimensional semiconductors are interrelated. For example, an increase in σ could result in a decrease in S, and also increase the carrier contribution to κ, which make it very difficult to achieve the improvement of ZT value as a whole.[18] In recent years, nanostructure design and nanocompositing opens another promising direction for the further optimization of conventional thermoelectric materials. Besides the optimization of conventional thermoelectric alloys,[18,30] such as Bi_2Te_3, PbTe, etc., thermoelectric performances of organic polymers have also received significant improvement by compositing the conductive organic polymers with inorganic nanowires or nanoparticles. Among these composites, CNTs/polyaniline (PANI) composite has received extensive attentions due to its easy fabrication and low costs.[14−16] In such composites, PANI coats around CNTs through π bounds, forming a kind of one-dimensional concentric cable nano structure. The composite possesses better thermoelectric property than either of its parent components due to the uniformly fabricated nanostructures.

Received: June 13, 2011
Accepted: December 1, 2011
Published: December 1, 2011

   dx.doi.org/10.1021/am201330f | ACS Appl. Mater. Interfaces 2012, 4, 81−86

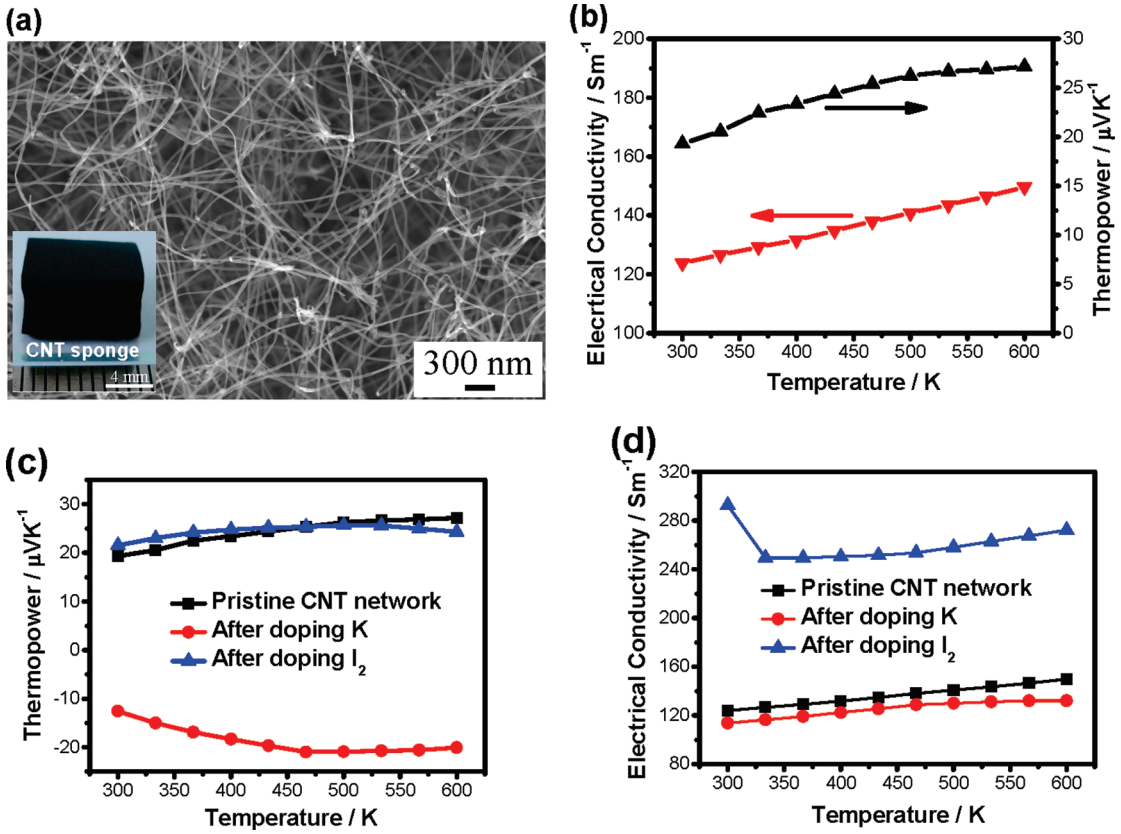

Figure 1. Microstructure and electrical transportation properties of the CNT network: (a) SEM image of the CNTs showing network structures, inset is the picture of an as-grown 3D CNT network; (b) electrical conductivity and thermopower of pristine CNT network in the temperature range of 300−600 K; (c) thermopower of the CNT network after doping K and I_2; (d) electrical conductivity of the CNT network after doping K and I_2.

However, macroscopically CNTs most commonly manifest the aggregate powder configuration, which cause a crucial dispersing problem of the CNTs because it is very easy to twist together and aggregate.[15,16] Recently, a kind of porous spongelike multiwall CNT network was synthesized by chemical vapor deposition.[19] The 3D CNT network as a nanoporous materials are original macroscopic structure based on three-dimensional CNT network (3D CNT network) with the porosity of above 98%.[6] This structure makes it a promising template to fabricate nanocomposites of CNTs with organic polymers that avoid the conventional dispersion problem of CNT.[29]

In this paper, the thermal and electrical transportation properties of the 3D CNT network have been investigated systematically. Donor and acceptor doping processes are used to modify the electrical transportation properties of pristine 3D CNT network. On the basis of the structure of 3D CNT network, a flexible polyaniline (PANI)/CNT composites were also fabricated, which shows significantly improved thermoelectric performance compared with both of its pristine parent components. It is hoped that the 3D CNT network template will contribute to the development of CNT-based composites in potential organic thermoelectric areas.

2. EXPERIMENTAL SECTION

2.1. Fabrication of the 3D CNT Network. The 3D CNT network has been fabricated using CVD according to our previous reports.[19] In brief, ferrocene powders were dissolved in 1,2-dichlorobenzene to make a solution at a concentration of 0.06 g/mL, which was then continuously injected into the CVD furnace at a constant feeding rate of 0.13 mL/min. The reaction temperature was 860 °C. Carrier gas of Ar and H_2, was flowing at a rate of 2000 and 300 mL/min, respectively.

2.2. Measurements of Electrical and Thermal Properties. For electrical transportation properties measurements, the CNT network were cut into rectangular bars with the approximate dimensions of 2 × 4 × 10 mm^3, maintaining its original density. Measurements of electrical conductivity and thermopower were carried out using ZEM-3 (ULVAC-RLKO) under the temperature range of 300 - 600 K. To measure the thermal conductivity of CNT network, both laser flashing and hotdisk methods have been applied: (1) In laser flashing method, the measurement of thermal diffusivity (λ) was carried out in Ar atmosphere under either normal pressure around 1 atm or low pressure around 20 Pa (Netzsch LFA 427), and the measurement was performed in the temperature range of 300−600 K. The sample of CNTs was cut into disk shape (diameter: 10 mm, thickness: 2 mm), and sprayed with graphite in each surface when carrying out the thermal diffusivity measurement. The heat capacity C_p of the CNT network was measured by differential scanning calorimetry (PE DSC-2C) in the temperature range of 300 - 500 K. Thermal conductivity κ was calculated from the relationship $\kappa = \rho\lambda C_p$, where λ is the thermal diffusivity coefficient, C_p is the heat capacity, and ρ is the density of the material. (2) The hot-disk measurement has been carried out using a standard device(ISO 22007−2:2008)with self-made liquid heating and vacuum systems. Thermal conductivities under either normal pressure around 1 atm or under low pressure around 20 Pa have been measured.

dx.doi.org/10.1021/am201330f | ACS Appl. Mater. Interfaces 2012, 4, 81−86

2.3. Doping of K and I_2. The doping K or I_2 is by gas fuming method. The gas fuming process has been carried out by sealing the 3D CNT network into a quartz tube under vacuum atmosphere together with the solid gas source of K and I_2, respectively (see the Supporting Information, Figure S1). The solid gas source was placed in a graphite crucible, and the CNTs were placed in a shelf above the crucible. The fuming conditions are under 400 °C for 20 h for K, or under 80 °C for 20 h for I_2.

2.4. Fabrication of PANI/CNT Network Composites. The fabrication of PANI/CNT network nanocomposites has been carried out by fully immersing the CNTs in solvent: 100 mL 1 M HCl (water/alcohol: 1:2) mixed with 2.5 mL ethanol. A certain amount of ammonium peroxidisulfate (APS) has been resolved in 20 mL 1 M HCl. Then the APS solution was slowly added dropwise to the aniline solution. The mixture was kept at 4 °C for 20 h for complete reaction. Finally, the PANI-coated CNT network was washed with deionized water and acetone, dried in a vacuum, and pressed into solid with density around 0.8 g/cm^3.

3. RESULTS AND DISCUSSION

As-fabricated 3D CNT network maintains spongelike construction with extremely low density around 10 mg/cm^3 and high porosity of 99%, as showing in Figure 1a inset. From further SEM observation (Figure 1a), the 3D CNT network is composed of interconnected multiwall CNTs, which have diameters around 30 nm and lengths convinced as several micrometers. This special structure renders the 3D CNT network very high structural flexibility that can be twisted, bend, or pressed elastically. Also, the deformation can be either maintained or recovered by further treatments,[19] which makes it possible to be changed into different shapes needed. The electrical conductivity and thermopower of 3D CNT network are around 120 S/m and 18 μV/K at 300 K, as shown in Figure 1b. Both parameters show positive temperature coefficient with the rise of temperature up to 600 K. The positive thermopower indicates that hole is the main carrier in the pristine 3D CNT network. It might be caused by the doping effect of oxygen or nitrogen in the air atmosphere, and the thermopower was generated from resonance of density of state and electron−phonon interaction during the electrical transportation from interfaces of CNTs.[20]

The doping effect provides opportunities to further adjust the electrical properties of CNT net work.[20−24] The self-sustainable structure of 3D CNT network makes it more convenient to carry out the redoping process and directly investigate its electrical transportation properties using standard methods. Here, potassium and iodine were chosen as the donor and acceptor dopant for the redoping processes. After doping, the alkali metal is homogeneous coating on the surface of the CNTs and forming string of bead nanoparticle with the size of about 100 nm (see the Supporting Information, Figure S2). The electrical conductivity and thermopower of the 3D CNT network after redoping are shown in c and d in Figure 1. By potassium fuming, the thermopower became negative in the whole temperature range, which indicates a p−n transformation of the 3D CNT network. This transform is caused by the alkali metal donor doping, in which process potassium deposited or intercalated into the CNTs and donating electrons to the framework of the 3D CNT network.[20−22] In contrast, after iodine doping the electrical conductivity was enhanced more than one time while the thermopower did not change significantly. The initial fall of electrical conductivity from 300 to 350 K may be caused by the partially vaporization of iodine that deposited on the CNT surface, after which point the electrical conductivity continued similar increasing temperature dependence as the original 3D CNT network. The increase in the electrical conductivity could be caused by the acceptor doping. During the iodine fuming process, iodine vapor deposited or intercalated into the CNTs as $(I_3)^-$ and $(I_5)^-$ polyiodide chains, donating one extra hole per three or five iodine atoms to the valence band of the CNTs, thus enhancing the main carrier concentration and improved the electrical conductivity.[23,24]

The thermal conductivity of the 3D CNT network has been measured using both hot disk and laser flashing method in different air pressures. The details of hot disk method were illustrated in Figure S3 in the Supporting Information. The thermal conductivities of 3D CNT network measured using different methods were similar magnitude. It shows superlow thermal conductivity, which around 0.02 W/(m K) in low pressure around 20 Pa, and 0.035 W/(m K) in standard atmosphere at room temperature, as shown in Figure 2a. The thermal conductivity of the 3D CNT network is the lowest, compared other reported CNT macrostructures like aligned CNT array,[7] aligned CNT sheets,[25] SWCNT film[26] and CNT bulk[27] (see Table 1). More details about thermal diffusity and thermal capacity in laser flashing measurement are shown in Figure 2b. The extremely low thermal conductivity of the 3D

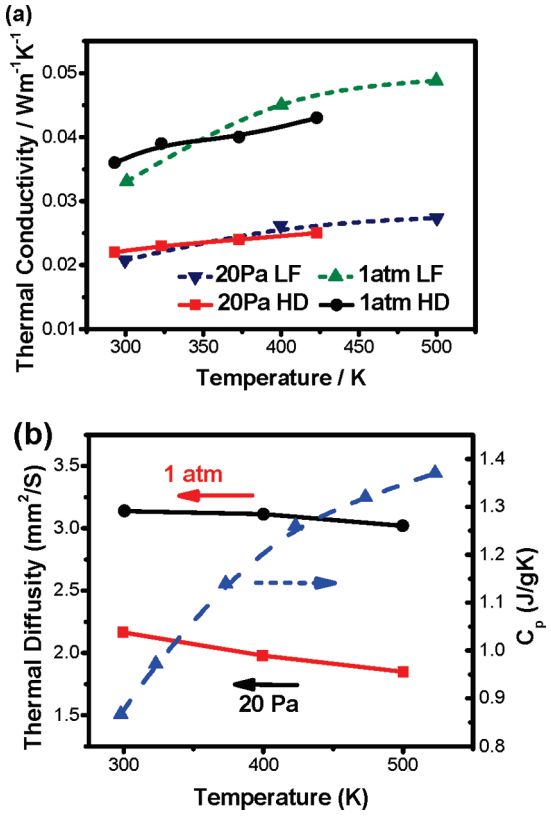

Figure 2. Thermal transportation properties of the 3D CNT network: (a) Thermal conductivity of pristine CNT network measured by methods of hot-disk (HD) and laser flashing (LF) in different pressure of 1 atm and 20 Pa. (b) Detailed temperature dependence of thermal diffusity of 3D CNT network at different pressures and the measured thermal capacity.

dx.doi.org/10.1021/am201330f | ACS Appl. Mater. Interfaces 2012, 4, 81−86

Table 1. Thermal Conductivity Comparison of the 3D CNT Network with Other Reported CNT Macrostructures

CNT types	thermal conductivity (W/mK)	ref
3D CNT network	0.035	present work
MWCNT array	0.06	7
MWCNT array (perpendicular direction)	0.5	7
MWCNT sheets (along CNT direction)	2.1	24
MWCNT sheets (along CNT direction)	50	24
SWCNT film (perpendicular CNT direction)	30	25
CNT bulk	4.2	26
MWCNT bundles	150	24
individual MWCNTs	600	24

CNT network should be attributed to its extremely low density because of the extremely high porosity of the unique three-dimensional framework structure. Generally speaking, two factors, heat exchange and heat convection, contribute to the thermal conductivity of the CNT network (radiation could be neglected in the relatively low temperature range). The difference of thermal conductivities at standard pressure and low pressure shows the contribution of gas convection to the total thermal conductivity of the 3D CNT network at standard air pressure and room temperature. On the basis of our result, at room temperature and standard pressure, gas convection contributed about 43% of the thermal conductivity at 300 K, whereas heat exchange through the framework of CNTs counted for the rest 57%. Combining with the electrical conductivity and estimating by Wiedemann–Franz law (as $\kappa_c = L_0\sigma T$, where L_0 is the Lorenz constant), it can be seen that lattice vibration contributed most to the heat exchange, since the carrier contribution was less than 3%.

The self-sustainable structure and conductive properties of the 3D CNT network makes it one of the best skeletons or template to carry out polymer/CNT compositing without the commonly encountered CNT dispersing problem. For demonstration here, polyaniline (PANI), which is a kind of conductive polymers, has been by in situ polymerized on to the surface of each single CNTs within the 3D network, as to modify the thermopower of as-produced 3D CNT network.

As the photograph in the Figure 3a inset shows, after the polymerization process, the as-produced PANI/3D CNT network composites maintained the self-sustainable structure. Unlike conventional PANI/CNT composites fabricated using powderlike CNT and cold-press molding,[16] as-produced composite here maintains the original flexibility of the 3D CNT network. It can be bent or pressed into different shapes, which can be maintained by being kept in a mold and dried. SEM images in Figure 3a,b further show that PANI chains coated on the outer walls of the CNTs, forming a concentric cable structure. This structure was formed through the following processes.[14−16] In the mixed solution for polymerization, aniline hydrochlorides are oxidized by ammonium peroxidisulfate (APS) to form insoluble polyaniline oligomers

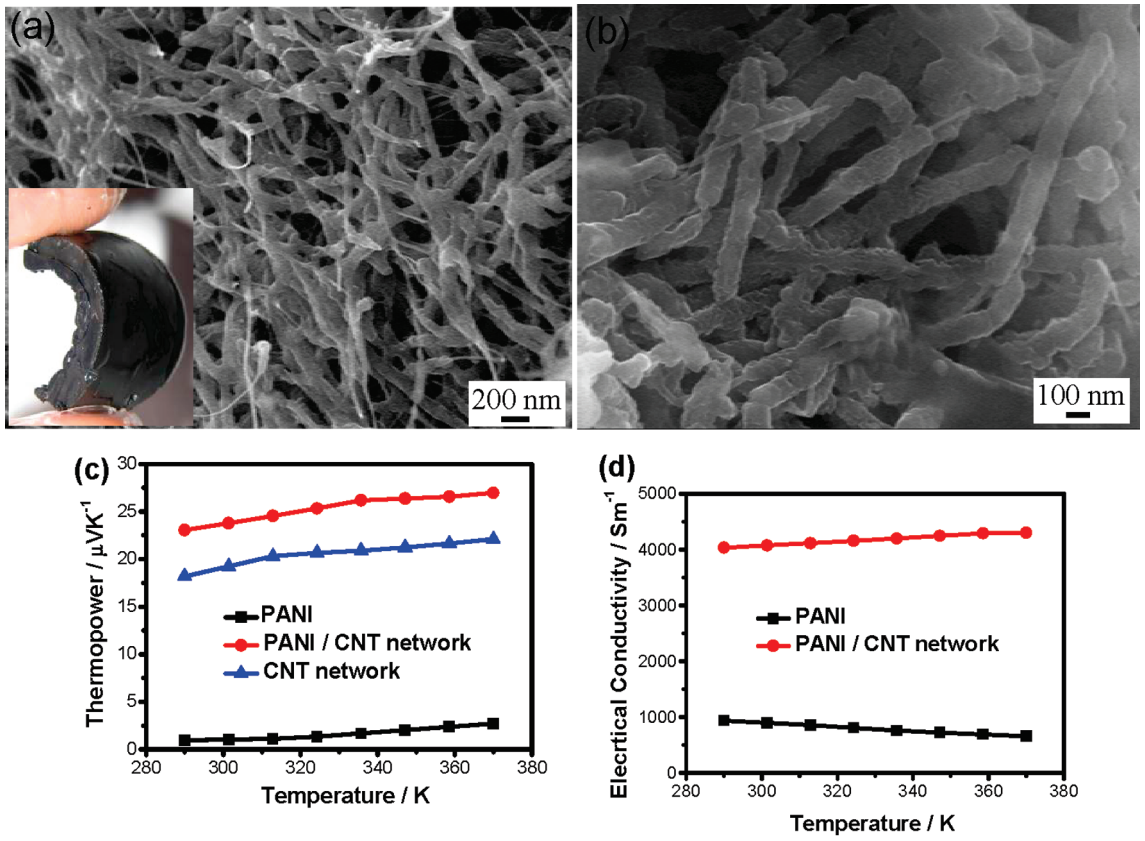

Figure 3. Modification the 3D CNTs network by coating PANI. (a, b) SEM image of the PANI/CNT composites in different magnification, with inset shown its macro photo; (c) thermopower of the PANI/CNT composites (44% mass content of CNT), compared with pure PANI and CNT network; (d) electrical conductivity of the PANI/CNT composites (44% mass content of CNT), compared with pure PANI.

dx.doi.org/10.1021/am201330f | ACS Appl. Mater. Interfaces 2012, 4, 81–86

Table 2. Detailed Thermoelectric Properties of 3D CNT Network, PANI, and PANI/CNT Network Composite at Room Temperature

samples	density (g/cm^3)	electrical conductivity (S/m)	thermopower (μV/K)	thermal conductivity (W/(m K))	ZT value
3D CNT network	0.011	123	18.2	0.02	6.0×10^{-4}
PANI	1.27	911	1.0	0.38	7.0×10^{-7}
PANI/3D CNT network Composite	0.8	4035	23.3	0.29	2.2×10^{-3}

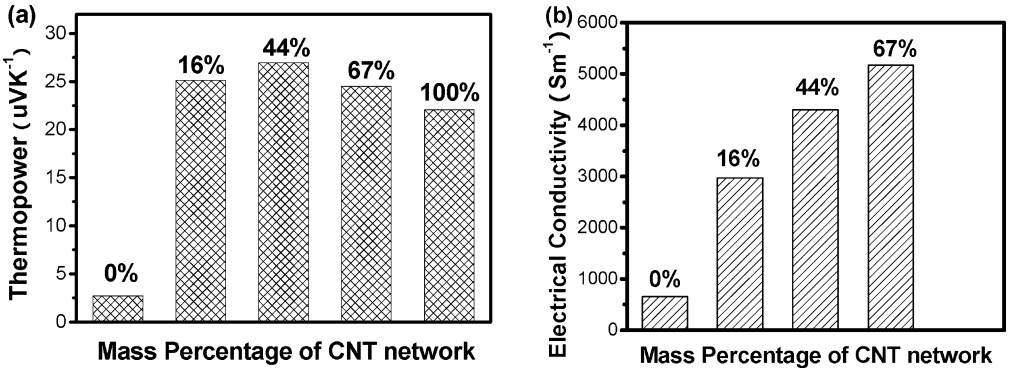

Figure 4. (a) Thermopowers and (b) electrical conductivities of the PANI/CNT network composites with different mass percent of 3D CNT network at 373 K.

and polymers, which interact strongly with the π-bonded surface of the CNTs and deposit at the surface of the CNTs, forming a tubular coating nano layer. Different proportion between PANI and CNT can be controlled adjusting the aniline concentration of the reacting solution.

As to better control the density and shape of the composite samples in electrical and thermal transport properties measurements, as-produced PANI/3D CNT network composites were pressed tightly to density around 0.8 g/cm^3, and cut into shapes of either rectangular bars in electrical transportation measurement or round disk (see more details in Figure S4 in the Supporting Information) in thermal conductivity measurement. As shown in Figure 3c, the thermopower of the composites exceeded either of its components in the whole temperature range, which manifests an unconventional composite advantage that is different with that in conventional 3D semiconductor theory, which maintains that the thermopower of composites through simply mixture could not exceed the highest thermopower of its components.[14,16] Compared with pure PANI, the electrical conductivity of the composites have been significantly improved (Figure 3d). Table 2 compares more details about thermoelectric properties of pure PANI, CNT network and PANI/CNT network composites (with 44% CNT content) at room temperature. It can be seen that after the pressing, both thermal and electrical conductivities of the composite sample were enhanced compared with pristine CNT network. Nevertheless, the electrical conductivity increased more significantly compared with that of thermal conductivity. Besides, the thermopower was also enhanced after compositing. As a result, the ZT value of the composite sample (0.0022) exceeded both pure PANI and pristine 3D CNT network. Figure 4 shows the electrical conductivities and thermopowers of the PANI/3D CNT network composites with different mass proportion of CNT/PANI. Electrical conductivities of the composite samples were enhanced with the increase of CNT content (electrical conductivity of pristine 3D CNT network was not compared due to its significantly different low density). Besides, it can be seen that the thermopower reached the maximum when the mass percentage of CNT reached about 44%, and all the composites have higher thermopower compared with pure PANI and 3D CNT network. Rather than the variation of carrier concentration, the enhancement of thermopower should be attributed to the design of nanostructure and interface. Because of the π-bond interaction of as-formed one-dimensional PANI with CNTs, the types of bounds (or state for transportation) at interface has been increased. When carriers hopping over these interfaces (CNT−CNT, CNT−PANI, or PANI−PANI), the π-bond would introduce additional states of the carriers. As a result, the thermopower could be enhanced.

On the basis of the above analysis, the 3D CNT network is a promising candidate in the fabrication of CNT/PANI composites, without encountering the conventional problem of CNT congregating. The thermoelectric performance of the composite improved significantly compared with both of its pristine components, while the structure and flexibility of the 3D CNT network has been retained.

4. CONCLUSIONS

In conclusion, the electrical and thermal transportation properties of a novel structured 3D CNT network have been systematically investigated. The thermal conductivity of the 3D CNT network is only 0.035 W/(m K) in standard atmosphere at room temperature, which is among the lowest compared with other reported CNT fabrications. The electrical properties of the 3D CNT network have been adjusted through convenient gas-fuming doping process. Through K fuming, the original p-type 3D CNT network converted to n-type, while I_2 gas fuming enhanced its electrical conductivity. On the basis of its self-sustainable homogeneous network structure, the 3D CNT network has been used as a template to composite with PANI. Through nanoscaled interface modification, the thermoelectric performance of the composites exceeds either of its components. At the same time, the structure and flexibility of the 3D CNT network can be retained. It is hoped that as-fabricated 3D CNT network would contribute to the development of low-cost organic thermoelectric area.

dx.doi.org/10.1021/am201330f | ACS Appl. Mater. Interfaces 2012, 4, 81−86

■ ASSOCIATED CONTENT

Supporting Information

Schematic illustration of the doping process of K or I_2 by gas fuming; SEM images of the CNT network after dopting K; Illustration of the self-made Hot-disk equipment used for thermal conductivity measurement; photos of the PANI/3D CNT network composite sample used for thermal conductivity measurement. This material is available free of charge via the Internet at http://pubs.acs.org.

■ AUTHOR INFORMATION

Corresponding Author

*E-mail: guixch@mail.sysu.edu.cn (X.G.); chenlidong@mail.sic.ac.cn (L.C.).

Author Contributions

‡These Authors contributed equally to this work.

■ ACKNOWLEDGMENTS

Financial support from National Natural Science Foundation of China (No. 50972159) and Program of Shanghai Subject Chief Scientist (09XD1404400) are greatly acknowledged. This work is also supported by National Science Foundation of China (NSFC) (Grants 51102286 and 51002190). Besides, assistance by Prof. Xiulan Zhang in Institute of semiconductors Chinese Academy of Sciences and National Natural Science Foundation of China (61076051) are also greatly acknowledged.

■ REFERENCES

(1) Tappan, B. C.; Steiner, S. A. I.; Luther, E. P. *Angew. Chem., Int. Ed.* **2010**, *49*, 4544−4565.

(2) Yu, Y.; Gu, L.; Zhu, C.; Zhu, C.; Tsukimoto, S.; Van Aken, P.; Maier, J. *Adv. Mater.* **2010**, *22*, 2247.

(3) Tang, Z.; Shen, S.; Zhuang, J.; Wang, L. *Angew. Chem., Int. Ed.* **2010**, *49*, 4603−4607.

(4) Xu, Y.; Sheng, K.; Li, C.; Shi, G. *ACS Nano* **2010**, *4*, 4324−4330.

(5) Futaba, D. N.; Miyake, K.; Murata, K.; Hayamizu, Y.; Yamada, T.; Sasaki, S.; Yumura, M.; Hata, K. *Nano Lett.* **2009**, *9*, 3302−3307.

(6) Gui, X.; Cao, A.; Wei, J.; Li, H.; Jia, Y.; Li, Z.; Fan, L.; Wang, K.; Zhu, H.; Wu, D. *ACS Nano* **2010**, *4*, 2320−2326.

(7) Jakubinek, M. B.; White, M. A.; Li, G.; Jayasinghe, C.; Cho, W. D.; Schulz, M. J.; Shanov, V. *Carbon* **2010**, *48*, 3947−3952.

(8) Lee, J.; Wang, L.; Kooi, S.; Boyce, M. C.; Thomas, E. L. *Nano Lett.* **2010**, *10*, 2592−2597.

(9) Davis, M. E. *Nature* **2002**, *417*, 813−821.

(10) Zhang, Q.; Zhao, M.; Liu, Y.; Cao, A.; Qian, W.; Lu, Y.; Wei, F. *Adv. Mater.* **2009**, *21*, 2876.

(11) Gibson, L. J. *J. Biomech.* **2005**, *38*, 377−399.

(12) Li, X.; Zhu, G.; Dordick, J. S.; Ajayan, P. M. *Small* **2007**, *3*, 595−599.

(13) Halonen, N.; Rautio, A.; Leino, A.; Kyllonen, T.; Toth, G.; Lappalainen, J.; Kordas, K.; Huuhtanen, M.; Keiski, R. L.; Sapi, A.; et al. *ACS Nano* **2010**, *4*, 2003−2008.

(14) Meng, C.; Liu, C.; Fan, S. *Adv. Mater.* **2010**, *22*, 535.

(15) Zhang, X.; Zhang, J.; Wang, R.; Liu, Z. *Carbon* **2004**, *42*, 1455−1461.

(16) Yao, Q.; Chen, L.; Zhang, W.; Liu, F.; Sheng, C.; Chen, X. *ACS Nano* **2010**, *4*, 2445−2451.

(17) Kim, D.; Kim, Y.; Choi, K.; Grunlan, J.; Yu, C. *ACS Nano* **2010**, *4*, 513−523.

(18) Dresselhaus, M. S.; Chen, G.; Tang, M. Y.; Yang, M. Y.; Lee, H.; Wang, D. Z.; Ren, Z. F.; Fleurial, J. P.; Gogna, P. *Adv. Mater.* **2007**, *19*, 1043−1053.

(19) Gui, X.; Wei, J.; Wang, K.; Cao, A.; Zhu, H.; Jia, Y.; Shu, Q.; Wu, D. *Adv. Mater.* **2010**, *22*, 617−621.

(20) Derycke, V.; Martel, R.; Appenzeller, J.; Avouris, P. *Appl. Phys. Lett.* **2002**, *80*, 2773−2775.

(21) Javey, A.; Tu, R.; Farmer, D. B.; Guo, J.; Gordon, R. G.; Dai, H. *Nano Lett.* **2005**, *5*, 345−348.

(22) Li, Y. F.; Hatakeyama, R.; Kaneko, T. *Appl. Phys. A: Mater. Sci. Process.* **2007**, *88*, 745−749.

(23) Miyajima, N.; Dohi, S.; Akatsu, T.; Yamamoto, T.; Yasuda, E.; Tanabe, Y. *Carbon* **2002**, *40*, 1533−1539.

(24) Fan, X.; Dickey, E. C.; Eklund, P. C.; Williams, K. A.; Grigorian, L.; Buczko, R.; Pantelides, S. T.; Pennycook, S. J. *Phys. Rev. Lett.* **2000**, *84*, 4621−4624.

(25) Aliev, A. E.; Lima, M. H.; Silverman, E. M.; Baughman, R. H. *Nanotechnology* **2010**, *21*, 0357093.

(26) Itkis, M. E.; Borondics, F.; Yu, A. P.; Haddon, R. C. *Nano Lett.* **2007**, *7*, 900−904.

(27) Zhang, H. L.; Li, J. F.; Yao, K. F.; Chen, L. D. *J. Appl. Phys.* **2005**, *97*, 11431011.

(28) Yu, C.; Kim, Y. S.; Kim, D.; Grunlan, J. C. *Nano Lett.* **2008**, *8*, 4428−4432.

(29) Gui, X.; Li, H.; Zhang, L.; Jia, Y.; Liu, L.; Li, Z.; Wei, J.; Wang, K.; Zhu, H.; Tang, Z.; Wu, D.; Cao, A. *ACS Nano* **2011**, *5*, 4276−4283.

(30) Chen, J.; Zhou, X.; G. Snyder, J.; Uher, C.; Chen, N.; Wen, Z.; Jin, J.; Dong, H.; Qiu, P.; Zhou, Y.; Shi, X.; Chen, L. *Chem. Commun.* **2011**, *47*, 12173−12175.